SHM
Structural Health Monitoring

Online Identification of Linear Time-varying Stiffness of Structural Systems by Wavelet Analysis

Biswajit Basu,[1,*] Satish Nagarajaiah[2] and Arunasis Chakraborty[1]

[1]*Department of Civil, Structural and Environmental Engineering*
Trinity College Dublin, Ireland
[2]*Department of Civil and Environmental Engineering & Mechanical Engineering and Materials Science, Rice University, USA*

An online identification of variation of stiffness in structural systems has been presented in this study. The proposed technique is based on wavelet analysis. The time-frequency characteristics of the wavelets have been used in the formulation of online identification. The basis function used is a modified version of the Littlewood–Paley wavelet. The bases generated from this wavelet at different scales have the advantage of non-overlapping frequency bands which has been utilized in the frequency tracking algorithm. Further, an algorithm for detection of variation in modes shapes in time-varying linear multi-degree-of-freedom (MDOF) systems has been developed. Several types of changes in stiffness, such as a sudden jump, a ramp (gradual) change, or a sudden change with subsequent restoration of stiffness have been considered as illustrative examples in case of single-degree-of-freedom (SDOF) and MDOF systems. It has been found that the proposed technique for wavelet based online identification is efficient in tracking different types of cases considered and has potential for application in adaptive control.

Keywords online identification · wavelets · L–P basis · stiffness varying systems

1 Introduction

System identification of structures has emerged as an interesting and important problem in the last two decades. A significant amount of research has been carried out in relation to identification of structural dynamic systems, which includes research by Beck [6], Doebling et al. [10], Ghanem and Shinuzoka [12], Hart and Yao [16], Kozin and Natke [20], Lin et al. [22], Shinuzoka and Ghanem [35], amongst others. Recently, active and semi-active control of structures has received considerable attention by numerous researchers such as Nagarajaiah et al. [25], Spencer and Nagarajaiah [37], Spencer et al. [40], Sae-Ung and Yao [42], Wu and Yang [47], Yang and Samali [48], Yang et al. [49–52], to mention a few. Effective implementation of these control schemes requires online identification of structural systems.

For a single-degree-of-freedom (SDOF) system, the most important parameter of the

*Author to whom correspondence should be addressed.
E-mail: basub@tcd.ie
Figures 1–4 and 6–12 appear in color online: http://shm.sagepub.com

Los Angeles, London, New Delhi and Singapore
Vol 7(1): 0021–16
[1475-9217 (200803) 7:1;21–16 10.1177/1475921707081968]

structure to be identified is its stiffness or natural frequency. Similar information may be obtained through natural frequencies and mode shapes for a multi-degree-of-freedom (MDOF) structure. The information of stiffness and the variation of stiffness with time are of importance in designing control strategies e.g., in active and semi-active tuned mass dampers (TMDs) [37,39,53]. The methods for estimating parameters of a structural system may be broadly classified into two categories depending on whether these methods are based on data in time domain or the Fourier transform of the data in frequency domain. Several frequency domain methods have been used for successful identification of non-linear structural dynamic system including reverse path methods [7,32], identification through feedback of outputs [1], embedded sensitivity functions [54], and higher order frequency response functions [46]. The frequency domain methods though popular, due to their simplicity in application suffers from the drawback that they are based on average temporal information. Most of the time domain methods are also based on identifying models with time invariant parameters. However, several research efforts have also been aimed towards identifying and tracking time varying parameters either by recursive and other modified time domain techniques or by other methods including Hilbert/Gabor transformed analysis techniques (e.g., [11,15,18,19,22,23,26,30,41,44,45]). Masri and Caughey [24] proposed a nonparametric identification technique for nonlinear dynamic problems. Smyth et al. [38] had obtained online estimation of the parameters of MDOF non-linear hysteretic systems based on the measurement of restoring forces. Among the time-frequency analysis tools, wavelet analysis has gained popularity in identification of systems. Being capable of retaining local frequency content information and its variation with time and having the advantage of flexible windowing over short time Fourier transform, wavelet transform methods have become powerful as techniques to identify time varying and non-linear systems [2,3,13,14,17,21,31,33,34]. Wavelet analysis provides a variety of bases function to suit specific purposes. For example, Newland [27,28] used Harmonic wavelet for vibration analysis; Lardies and Gouttebroze [21] proposed a modified Morlet wavelet basis while Basu and Gupta [4,5] and Chatterjee and Basu [8,9] used a modified Littlewood–Paley (L–P) basis function for reasons suitable for specific applications.

While the wavelet analysis techniques have been successfully used mostly in offline identification of the time varying structural dynamic parameters of a system, it has the potential of online identification, using time-frequency properties. The online identification of system parameters can be achieved in a simple and computationally straightforward way by using wavelet analysis useful for adaptive control application, which has not been explored much, so far.

In this study, a wavelet based online identification of stiffness of structural system has been proposed. A modified L–P wavelet basis with wavelet packets has been used in the proposed algorithm. Formulations for a SDOF system and MDOF system have been presented. Illustrations have been used to show the efficiency of the proposed tracking algorithm.

2 Wavelet Based Online Identification

The online identification problem for a linear SDOF system is first considered. The natural frequency of the system is tracked.

2.1 Online Identification of SDOF System

A linear SDOF system with time varying stiffness is considered here. The equation of motion of this system may be represented as:

$$\ddot{x} + 2\eta\omega_n(t)\dot{x} + \omega_n^2(t)x = f(t) \tag{1}$$

where, $\omega_n(t)$ is the time varying natural frequency, η is the damping ratio, and $x(t)$ is the displacement response due to the excitation $f(t)$. The parameter, $\omega_n(t)$ is a time varying function with discontinuities at finite number of points. Hence, the domain in time can be segmented in several intervals with the time indices

$t_0 < t_1 < t_2 < \cdots < t_n$ such that the natural frequency $\omega_{n_i}(t)$ within the interval $[t_{i-1}, t_i]$ is a continuous function. This will lead to a sequence of time-varying linear equations each valid over an interval of time. The wavelet transform of the response $x(t)$ can be expressed as:

$$
\begin{aligned}
W_\psi x\big(a_j, b\big) &= \frac{1}{a_j}\int_{-\infty}^{+\infty} x(t)\psi\left(\frac{(t-b)}{a_j}\right)\mathrm{d}t \\
&\approx \frac{1}{\sqrt{a_j}}\int_{b-\varepsilon}^{b+\varepsilon} x(t)\psi\left(\frac{(t-b)}{a_j}\right)\mathrm{d}t
\end{aligned}
\tag{2}
$$

where, both $x(t)$ and the wavelet basis function $\psi(t)$ are real functions of time. In Equation (2), $\psi((t-b)/a_j)$ translates and scales the basis function $\psi(t)$ by a continuous parameter 'b' and a discrete parameter 'a_j', respectively. The scaling parameter is discretized in an exponential scale 'a_j' and the discretization is performed as $a_j = \sigma^j$, where σ is a scalar. The wavelet coefficient $W_\psi x\big(a_j, b\big)$ localizes information about the function $x(t)$ around '$t=b$' at a scale 'a_j' corresponding to the frequency band of the Fourier transform of $\psi((t-b)/a_j)$ i.e., $\hat{\psi}\big(a_j\omega\big)$. Since, $\psi((t-b)/a_j)$ is a decaying function centered around '$t=b$', it has the advantage that the integral in Equation (2) may be performed over a finite interval $[b-\varepsilon, b+\varepsilon]$ around '$t=b$' without much loss of information. The choice of ε would depend on the decay of $\psi((t-b)/a_j)$ or the related central frequency band corresponding to the scale a_j. Multiplying both sides of Equation (1) by $\psi((t-b)/a)$, integrating over $b-\varepsilon$ to $b+\varepsilon$, where $b \in [t_{i-1}-\varepsilon, t_{i+1}+\varepsilon]$, and if $\omega_{n_i}(t)$ is a relatively slowly varying function of time as compared to the fast decaying function $\psi((t-b)/a)$ centered around '$t=b$', $\omega_{n_i}(t)$ can be taken out of the integral as approximately a constant, evaluated around '$t=b$'. Further, using integration by parts (see [5, 43]) leads to

$$
W''_{\psi_j}x + 2\eta\omega_n(b)W'_{\psi_j}x + \omega_{n_i}^2(b)W_{\psi_j}x = W_{\psi_j}f \tag{3}
$$

for a particular band with a corresponding scale of a_j. In Equation (3), the prime denotes differentiation with respect to b and $W_{\psi_j}(.)$ for brevity represents $W_\psi(.)\big(a_j, b\big)$.

The modified L–P basis function (Basu and Gupta ([4], [5]) used as the basis function for analysis has a band-limited support in frequency domain. It is characterized by the Fourier transform given by

$$
\begin{aligned}
\hat{\psi}(\omega) &= \frac{1}{\sqrt{F_1(\sigma-1)}}, \quad F_1 \le |\omega| \le \sigma F_1 \\
&= 0 \quad \text{otherwise}
\end{aligned}
\tag{4}
$$

where, F_1 is the initial cut off frequency of the mother wavelet. Taking the inverse Fourier transform of Equation (4), the wavelet basis function is given by

$$
\psi(t) = \frac{1}{\sqrt{\pi F_1(\sigma-1)}} \cdot \frac{\sin(\sigma F_1 t) - \sin(F_1 t)}{t}. \tag{5}
$$

If the modified L–P basis function is used, then $\hat{\psi}\big(a_j\omega\big)$ is supported over $\big[\sigma F_1/a_j, F_1/a_j\big]$. As a consequence of the localization of the basis function in time (decay $\approx 1/t$) as compared to a non-localized harmonic function, the frequency content is supported over a band $\big[\sigma F_1/a_j, F_1/a_j\big]$. Hence, from Equation (2), it follows that the frequency content of the signal $\hat{W}_{\psi_j}x$, a function of b, will be also supported over $\big[\sigma F_1/a_j, F_1/a_j\big]$. Thus, $W_{\psi_j}x$ can be assumed to be narrow banded with the central frequency $\omega_{0j} = ((\sigma+1)/2)\cdot(F_1/a_j)$, which is the central frequency of the jth band and can be represented as:

$$
W_{\psi_j}x(b) = A_j(b)e^{-i\left(\omega_{0_j}b + \phi_j\right)}. \tag{6}
$$

In Equation (6), $A_j(b)$ is the amplitude or the modulus of the wavelet coefficient function of $x(t)$, $W_{\psi_j}x(b)$, and φ_j is the phase. Substituting Equation (6) in Equation (3) leads to

$$
W_{\psi_j}x(b) = H_j(b)W_{\psi_j}f(b) \tag{7}
$$

where,

$$
H_j(b) = \frac{1}{\left[\omega_{n_i}^2(b) - \omega_{0j}^2\right] + i\left[2\eta\omega_{n_i}(b)\omega_{0_i}\right]}. \tag{8}
$$

Squaring both sides of Equation (7), and integrating over $b-\varepsilon$ to $b+\varepsilon$, gives the local energy content of $x(t)$ in the jth band around b, $E_j x(b)$. If $f(t)$ is assumed to be broad banded, the energy content of $f(t)$ in any band would be comparable in the order of magnitude to the energy content in any other band. It follows that

$$E_j x(b) \propto \frac{1}{a_j}\int_{b-\varepsilon}^{b+\varepsilon} |W_{\psi_j} x(\bar{b})|^2 \mathrm{d}\bar{b} \propto \frac{1}{a_j}\int_{b-\varepsilon}^{b+\varepsilon} |H_j(\bar{b})|^2 \mathrm{d}\bar{b} \tag{9}$$

if $\omega_{n_i}(b)$ is assumed to be invariant over the window $[b-\varepsilon, b+\varepsilon]$. It can be noticed that the expression in the denominator in Equation (9) is minimum when $\omega_{n_i}(b)$ is close to ω_{0j}. Alternatively, it may be stated that $E_j x(b) \propto \int_{b-\varepsilon}^{b+\varepsilon} \left|W_{\psi_j} x(b)\right|^2 \mathrm{d}b/a_j$ is maximum when $\omega_{n_i}(b) \in \left[\sigma F_1/a_j, F_1/a_j\right]$ for a lightly damped system ($\eta \ll 1$), which indicates that $\omega_{n_i}(b)$ is contained in the jth band. Hence, the energies in the different bands would satisfy the inequality $E_1 x(b) < \cdots < E_{j-1} x(b) < E_j x(b) > E_{j+1} x(b) > \cdots > E_N x(b)$ if $\omega_{n_i}(b) \in \left[\sigma F_1/a_j, F_1/a_j\right]$ where N is the total number of bands. Thus it may be concluded that provided the bands are narrow, $\omega_{n_i}(b) \approx \omega_{0j}$, if the jth band contains the maximum energy.

If the estimation of $\omega_{n_i}(b)$ is desired with a still further precision then the technique of wavelet packet can be used. This is an extension of the wavelet transform to provide further level-by-level time-frequency description and can be easily applied for L–P basis. The estimation of the time varying parameter $\omega_{ni}(b) \in \left[\sigma F_1/a_j, F_1/a_j\right]$ is refined by further re-dividing the band. The frequency band for the pth sub-band within the original jth band is in the interval $\left[\delta^{p-1} F_1/a_j, \delta^p F_1/a_j\right]$. The wavelet coefficient is denoted by $W_{\psi_{sp}} x(a_j, b)$. Using these wavelet coefficients, estimating the relative energy in the sub-bands and using Equation (16), the parameter $\omega_{ni}(b)$ can be obtained more precisely.

2.2 Online Identification of MDOF System

A linear MDOF system with m degrees of freedom represented by

$$[M]\{\ddot{X}\} + [C(t)]\{\dot{X}\} + [K(t)]\{X\} = \{R\}f(t) \tag{10}$$

is considered where, $[M]$, $[C(t)]$, and $[K(t)]$ are the mass, time varying damping, and time varying stiffness matrices, respectively; $\{R\}$ is the influence vector for forces at different degrees of freedom and $f(t)$ is a forcing function. The displacement response vector is denoted by $\{X(t)\}$. If the elements $K_{lj}(t); l, j = 1, \ldots, m$ in the stiffness matrix have discontinuities at a finite number of points, then it is possible to divide the time in several segments with indices arranged as $t_o < t_1 < t_2 < \cdots < t_n$ such that all $K_{lj}(t); l, j = 1, \ldots, m$ are continuous function in $[t_{i-1}, t_i]$. Further, it is assumed that the variations of all $K_{lj}(t)$ are slower than the fundamental (lowest) frequency of the system (corresponding to the longest period). It subsequently follows that assuming a variation of $\{X(t)\}$ with slowly varying amplitude $\{\phi(t)\}_i^k$ and slowly varying frequency $\omega_{k_i}(t)$ at the kth mode, in the time interval $[t_{i-1}, t_i]$, the displacement vector and its derivatives can be represented by

$$\{X(t)\} = \{\phi(t)\}_i^k e^{i\omega_{k_i}(t)t} \tag{11a}$$

$$\{\dot{X}(t)\} \approx i\omega_{k_i}(t)\{\phi(t)\}_i^k e^{i\omega_{k_i}(t)t} \tag{11b}$$

$$\{\ddot{X}(t)\} \approx -\omega_{k_i}^2(t)\{\phi(t)\}_i^k e^{i\omega_{k_i}(t)t}. \tag{11c}$$

Substitution of Equations (11a)–(11c) in the homogeneous free vibration equation corresponding to Equation (10) leads to the time-varying eigenvalue problem with eigenvalues $\omega_{k_i}^2(t)$ and eigenvectors $\{\phi(t)\}_i^k; k = 1, 2, \ldots, m$. If the system in Equation (10) is assumed to be classically damped, then substituting $\{X(t)\}$ in terms of modal responses, $z_k(t)$, using

$$\{X(t)\} = [\phi(t)]_i\{z_k(t)\}; \quad t \in [t_{i-1}, t_i] \tag{12}$$

in Equation (10) and pre-multiplying both side by $[\phi(t)]_i^{\mathrm{T}} = [\{\phi(t)\}_i^1\{\phi(t)\}_i^2 \ldots \{\phi(t)\}_i^k]$, leads to the following m modal uncoupled time varying equations

$$\ddot{z}_k(t) + 2\eta_k\omega_{k_i}(t)\dot{z}_k(t) + \omega_{k_i}^2(t)z_k(t) = f_k(t); \quad k = 1, 2, \ldots, m; \quad t \in [t_{i-1}, t_i]. \tag{13}$$

In Equation (13), η_k is the modal damping ratio, $\omega_{k_i}^2$ is the natural frequency in the kth mode in the interval $[t_{i-1}, t_i]$, and $f_k(t)$ is the modal force given by

$$f_k(t) = \alpha_i f(t) \tag{14}$$

where, α_i is a scalar defined by

$$\alpha_i = \frac{\{\phi^k(t)\}_i^T \{R\}}{\{\phi^k(t)\}_i^T [M] \{\phi^k(t)\}_i^T}. \tag{15}$$

Considering the rth degree of freedom with the displacement response state denoted by $X_r(t)$ and wavelet transforming Equation (12) yields

$$W_\psi x_r(a_j, b) = \sum_{k=1}^{m} W_\psi \left[\phi_{r_i}^k(t) z_k(t)\right](a_j, b); \quad r = 1, 2, \ldots, m. \tag{16}$$

Since the functions, $\phi_{r_i}^k(t)$ are slowly varying compared to $z_k(t)$, in evaluating the integral for wavelet transformation in Equation (16), $\phi_{r_i}^k(t)$ can be approximated by $\phi_{r_i}^k(b)$, as $\psi((t-b)/a_j)$ is localized and hence $\phi_{r_i}^k(b)$ can be taken out of the integral. This leads to

$$W_\psi x_r(a_j, b) = \sum_{k=1}^{m} \phi_{r_i}^k(b) W_\psi z_k(a_j, b); \quad r = 1, 2, \ldots, m. \tag{17}$$

Following similar steps as for the SDOF system in Section 2.1, it can be concluded that for each of the modal equation given by Equation (13)

$$E_j z_k(b) \propto \frac{1}{a_j} \int_{b-\varepsilon}^{b+\varepsilon} \left|W_{\psi_j} z_k(b)\right|^2 \mathrm{d}b \tag{18}$$

where, the parameter $\omega_{k_i}(b)$ is invariant over $[b-\varepsilon, b+\varepsilon]$. If the forcing function is assumed to be broad banded as was assumed in the case of SDOF system, then by calculating the relative energies in different bands and comparing, it may be inferred that

$$E_{j_K} z_k(b) \propto \frac{1}{a_{j_K}} \int_{b-\varepsilon}^{b+\varepsilon} \left|W_{\psi_j} z_k(b)\right|^2 \mathrm{d}b = \max\{E_N z_j(b)\}, \quad \forall j = 1, \ldots, N \tag{19}$$

where N is the number of energy bands. It implies that $\omega_{k_i}(b)$ corresponding to the kth mode is in the j_kth band i.e., $\omega_{k_i}(b) \in \left[F_1/a_{j_K}, \sigma F_1/a_{j_K}\right]$ and can be approximated as:

$$\omega_{k_i}(b) \approx \omega_{0_{jk}} = \frac{\sigma+1}{2} \cdot \frac{\pi}{a_{j_k}} \tag{20}$$

for a lightly damped system (with $\eta_k \ll 1$), where $\omega_{0_{jk}}$ is the central frequency of the j_kth band. Let the parameters $\omega_{1_i}(b), \omega_{2_i}(b), \ldots, \omega_{m_i}(b)$ be contained in the bands with scale parameters identified by indices $j_1, j_2, \ldots, j_m$, respectively. Since, the response in the kth mode, i.e., j_kth band is narrow banded with frequency around $\left[F_1/a_{j_K}, \sigma F_1/a_{j_k}\right]$, it follows that the bands not containing the natural frequency leads to insignificant energy i.e.,

$$E_j z_k(b) \ll E_{j_k} z_k(b) l; \quad \forall k = 1, 2, \ldots, m; \quad j \neq j_k. \tag{21}$$

It follows from Equations (19) and (21),

$$\left|W_{\psi_j} z_k(a_j, b)\right| \ll \left|W_{\psi_{j_k}} z_k(a_j, b)\right|, \quad j \neq j_k; k = 1, 2, \ldots, m \tag{22}$$

which leads to the approximation

$$\left|W_{\psi_j} z_k(a_j, b)\right| \approx 0 \quad \text{if } j \neq j_k; k = 1, 2, \ldots, m. \tag{23}$$

Using Equation (23) in Equation (17) yields

$$W_\psi x_r(a_j, b) \approx \phi_{r_i}^k(b) W_\psi z_k(a_j, b) \quad \text{if } j = j_k;\ k = 1, 2, \ldots, m$$
$$\approx 0 \quad \text{if } j \neq j_k \tag{24}$$

leading to

$$E_j x_r(b) \propto \frac{1}{a_j} \int_{b-\varepsilon}^{b+\varepsilon} \left[\phi_{r_i}^k(b)\right]^2 \left|W_\psi z_k(a_{j_k}, b)\right|^2 \mathrm{d}b \quad \text{if } j \neq j_k;\ k = 1, 2, \ldots, m. \tag{25}$$

Thus, the 'm' bands with the 'm' natural frequency parameters $\omega_{k_i}(b); k = 1, \ldots, m$ correspond to m local maxima in the variation of

$E_j x_r(b)$ [or its proportional quantity $(1/a_j)\int_{b-\varepsilon}^{b+\varepsilon}|W_\psi x_r(b)|^2\,db$] with different values of the band parameter 'j'. It can be represented by the inequalities

$$E_{j-1}x_r(b) < E_j x_r(b) > E_{j+1}x_r(b);\quad \forall j = j_k;\ k = 1, 2, \ldots, m \qquad (26)$$

if the modes are not too closely spaced. Once these bands are detected, the parameters $\omega_{k_i}(b)$ can be obtained as:

$$\omega_{k_i}(b) \approx \frac{\sigma+1}{2}\cdot\frac{F_1}{a_{j_k}};\quad k = 1, 2, \ldots, N \qquad (27)$$

over the interval $[b-\varepsilon, b+\varepsilon]$. The sub-band coding with wavelet packets could be applied if the parameters $\omega_{k_i}(b)$ are desired to be obtained with better precision as has been discussed in the section on the SDOF system.

Once the bands corresponding to the 'm' modes with the parameters $\omega_{k_i}(b)$ are obtained, the time varying mode shapes $\{\phi(t)\}_i^k$ could be found by considering the wavelet coefficients of $x_r(t)$ with the scale parameters, j_k and sub-band parameter p. These wavelet coefficients can be written as

$$W_{\psi_{sp}}x_r(a_j, b) = \phi_{r_i}^k(b)\,W_{\psi_{sp}}z_k(a_{j_k}, b). \qquad (28)$$

Now, considering two different states of response of the MDOF system with one considered as $r = 1$ (without the loss of generality), the ratio of wavelet coefficients of the considered states at the time instant $t = b$ (Equation (24) or (28)), gives the rth component of the time varying kth mode as

$$\pi_r^{j_k}(b) = \frac{W_{\psi_{sp}}x_r(a_{j_k}, b)}{W_{\psi_{sp}}x_1(a_{j_k}, b)} = \frac{\phi_r^k(b)}{\phi_1^k(b)}. \qquad (29)$$

Thus, computing these ratios for different states with $r = 1, 2, \ldots, m$ and assuming $\phi_1^k(b) = 1$ (without loss of generality), the time varying kth mode shape can be obtained.

The outlined procedure for obtaining the time varying natural frequencies and mode shapes could be shown to yield the same expressions if free or ambient vibrations induced due to an excitation with arbitrary initial conditions are considered.

3 Examples of Online Identification

For the purpose of illustration of the proposed algorithm for online identification of time varying SDOF and MDOF systems, first a band limited white noise excitation has been simulated. The range of frequencies is kept wide enough to cover the frequencies of the system to be identified. To maintain stationarity, the excitation has been generated by considering a number of cycles of an arbitrary number of discrete frequencies over the range so that the temporal mean square value is almost invariant. The excitation has been digitally simulated at a time step of $\Delta t = 0.0104$ s. For the frequency-tracking algorithm, a moving window of 400 time steps equal to 4.16 s has been chosen. The instantaneous frequency is identified based on the proposed formulation using wavelet analysis on the time histories of the response states and is updated at every time step. The identified frequency is assumed to be the central frequency of the frequency band for a particular identified scale of the L–P wavelet basis function.

Figure 1 shows the tracked frequency of a SDOF system with time-invariant natural frequency, $\omega_n = 9$ rad/s and damping ratio, $\eta = 5\%$. Since, a window of 4.16 s is used, the tracking starts after an initial period of 4.16 s. The value of the initial frequency of the first band of the mother wavelet, F_1 in Equation (8) is 8.25 rad/s and a value of the scaling constant, $\sigma = 1.2$ is used. Six bands are used in all and sub-band coding for packets are not used for this case. To investigate if a sudden or a sharp change in the natural frequency can be tracked, an example where the natural frequency of the SDOF system has been changed suddenly from 9 to 13.25 rad/s has been considered. Figure 2 shows how the natural frequency is tracked using the proposed method. As expected it requires a certain period of lag time to follow the change until it converges to the changed frequency which is the time-delay and is approximately equal to the time window (4.16 s) used for tracking. To further observe the

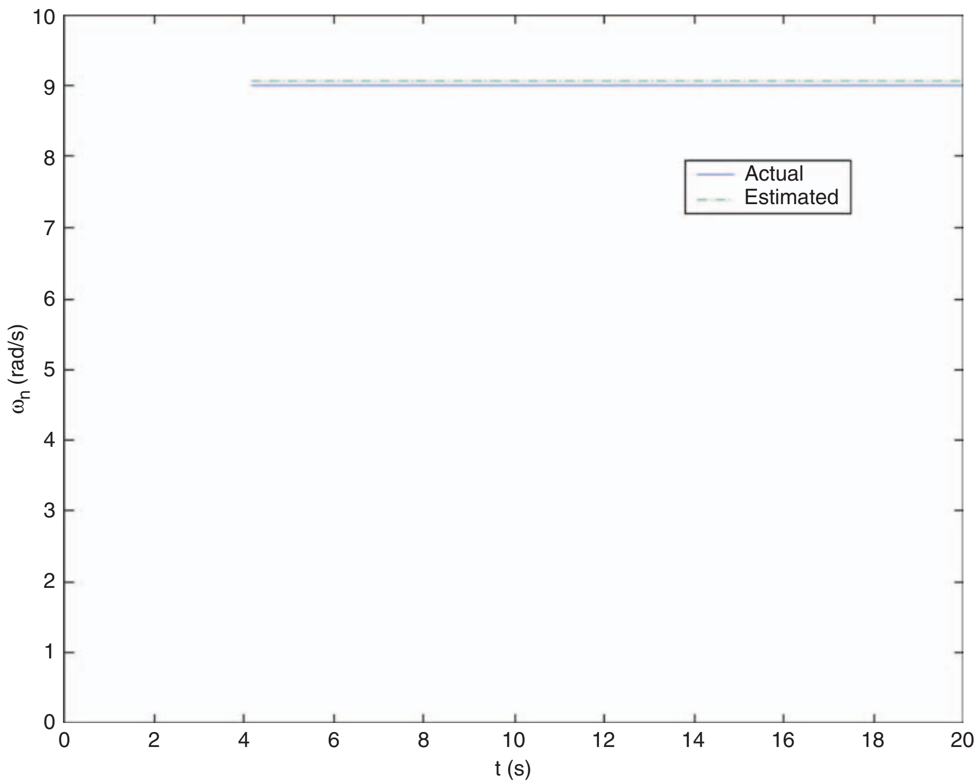

Figure 1 Online identification of natural frequency of a time invariant SDOF system.

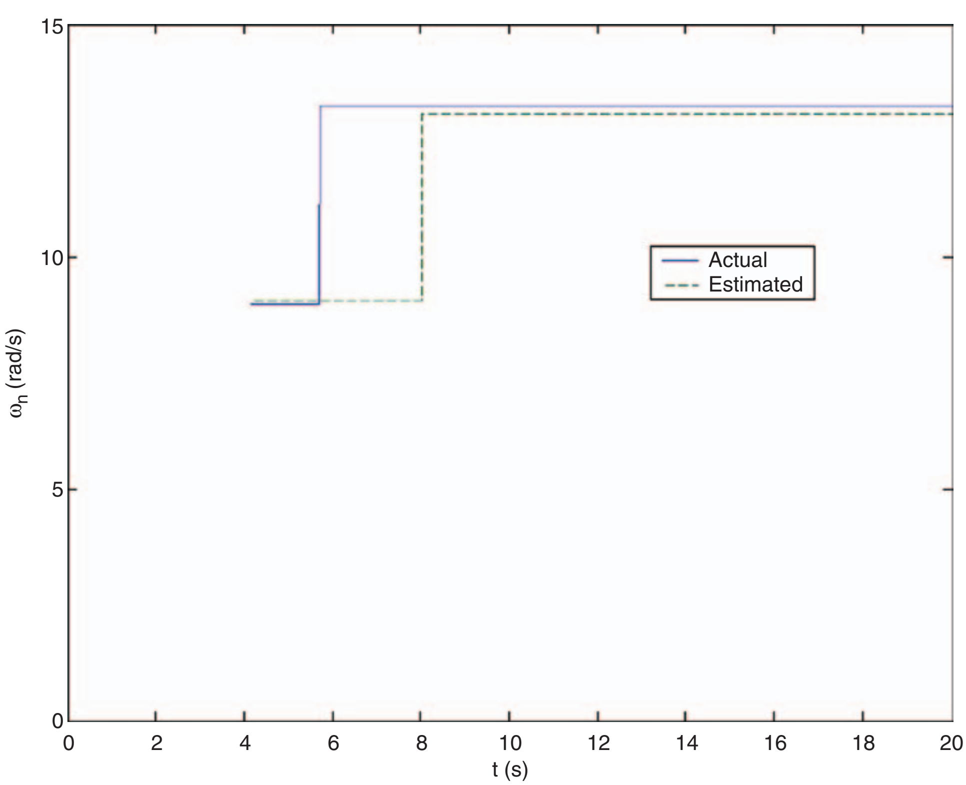

Figure 2 Tracking of sudden change in natural frequency of a SDOF system.

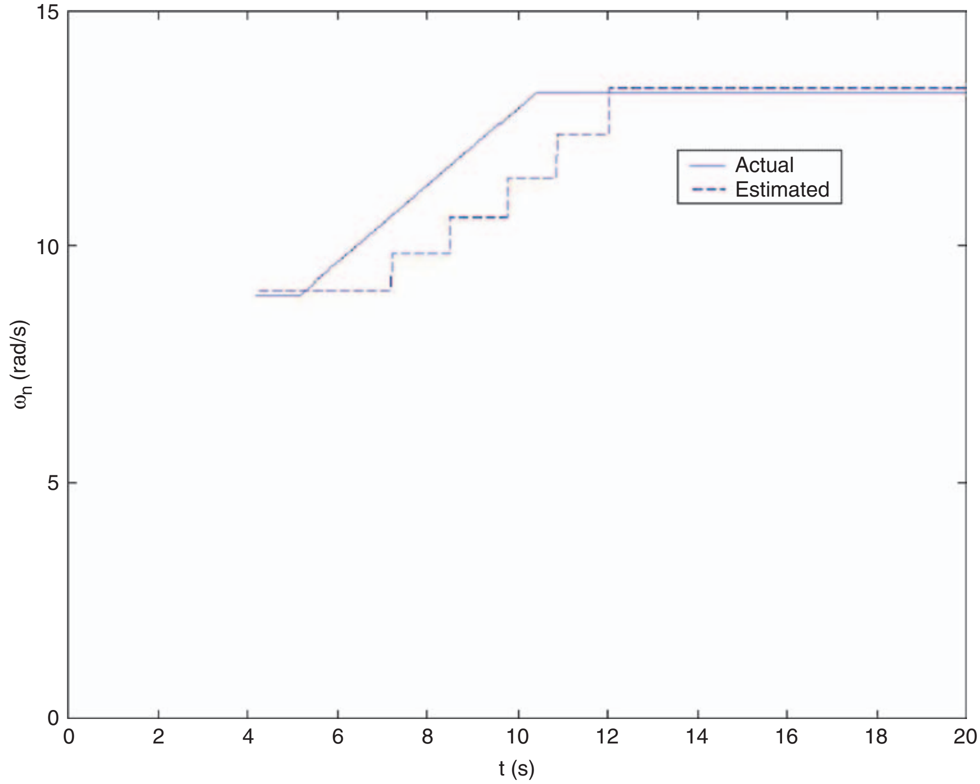

Figure 3 Tracking of change (ramp) in natural frequency of a SDOF system.

tracking ability of the method, a case where the change in the frequency of the SDOF system is not so sharp has been considered next. The natural frequency of the system is linearly changed in the form of a ramp from 9 to 13.25 rad/s over a period ranging over 5–10 s. Thus, apart from two discontinuities of slopes at 5 and 10 s, respectively, the variation of the frequency of the system is continuous with no discontinuity of slope. The frequency in this case can be tracked closely as seen in Figure 3. However, as six bands are used over the range of variation in frequency considered, the identification of the frequency occurs in five steps. The tracking can be more continuous by increasing the number of bands of frequencies considered for computation. To investigate if a relatively small change in stiffness can be tracked, a case where the natural frequency changes from 9 to 9.5 rad/s is considered and the results for successful tracking are shown in Figure 4 with a window width of 200 sampling points corresponding to a time delay of 2.08 s. For this, the parameters F_1 and σ are taken as 8.9 rad/s and 1.02, respectively. This indicates that the minimum change in stiffness that can be tracked is related to the value of σ and to identify a small change a relatively smaller value of σ will be required.

Next, to illustrate the application of the tracking methodology for MDOF systems an example of a 2 DOF system has been considered. The system considered is a shear-building model (as shown in Figure 5) with 2 DOF subjected to base excitation. The masses are lumped at the two nodes with the masses at first and second floors as $m_1 = 10$ unit and $m_2 = 15$ unit, respectively. The floor stiffness for the first and second floor are $k_1 = 2500$ unit and $k_2 = 4500$ unit, respectively. These parameters lead to the first and second natural frequencies, $\omega_1 = 9.04$ and $\omega_2 = 30.30$ rad/s, respectively. The first and the second mode shapes are $\{\phi_{11} \quad \phi_{21}\} = \{1 \quad 1.37\}$ and $\{\phi_{12} \quad \phi_{22}\} = \{1 \quad -0.48\}$, respectively. For the identification of the 2 DOF system, the parameters F_1 and σ are taken as 8.25 rad/s and 1.2, respectively. Figures 6 and 7 show the

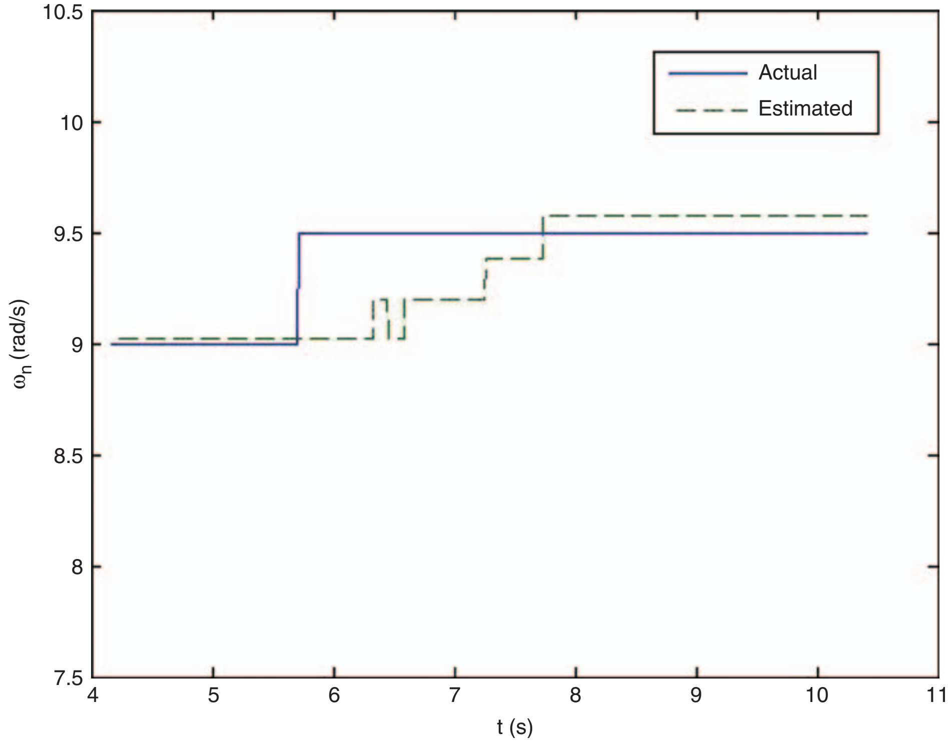

Figure 4 Tracking of small change in natural frequency of a SDOF system.

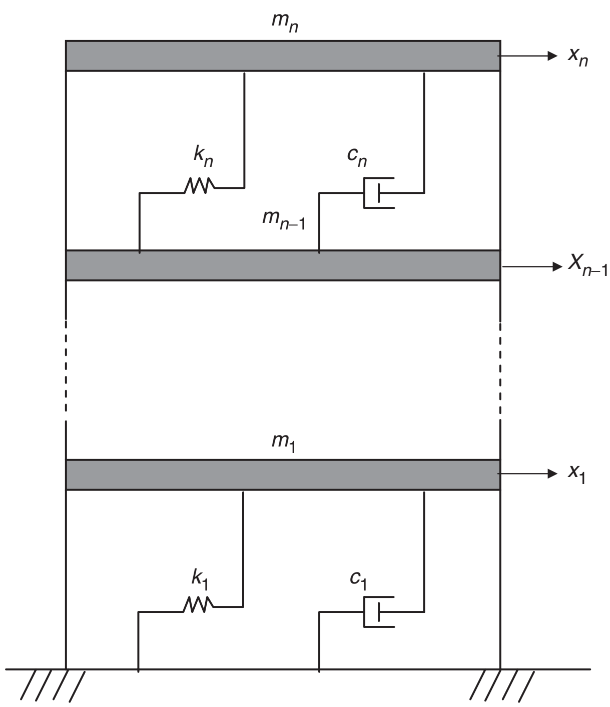

Figure 5 A MDOF shear building model.

tracking of the first natural frequency and the ratio ϕ_{21}/ϕ_{11} corresponding to the first mode shape (assuming $\phi_{11}=1$ without loss of generality). Similarly, Figures 8 and 9 show the tracking of the second natural frequency and the ratio ϕ_{22}/ϕ_{12} corresponding to the second mode shape (assuming $\phi_{12}=1$ without loss of generality). It can be observed that for the second mode shape, there is some fluctuation primarily in identifying the mode shape parameters. It is known that the identification problem becomes difficult for the last few modes of an MDOF system if these contain low energy or else if these are not excited. Hence, the second mode cannot be identified so accurately as the first mode for the 2 DOF system considered as the second mode has much lower participation factor when excited by base excitation.

For the purpose of verifying the mentioned cause of non-identification of the second mode shape in the 2 DOF system, an additional system (shear building model) with 5 DOF is considered. The lumped masses at the nodes from the first to the fifth floors are $m_1=30$ unit,

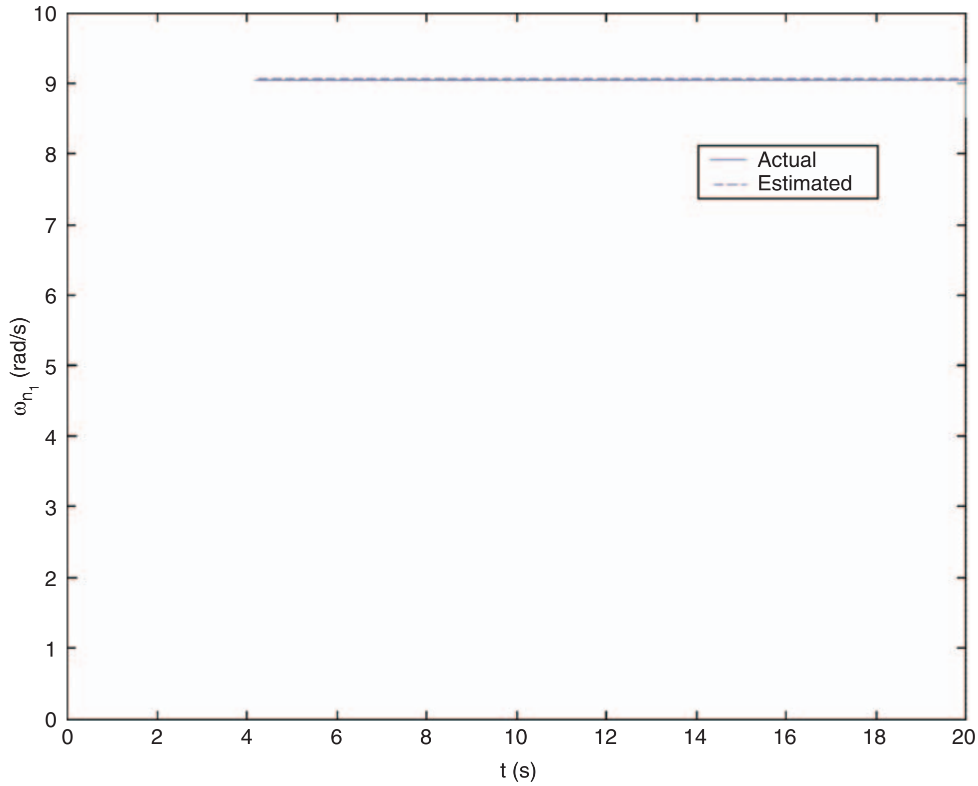

Figure 6 Online tracking of fundamental frequency of a 2 DOF system.

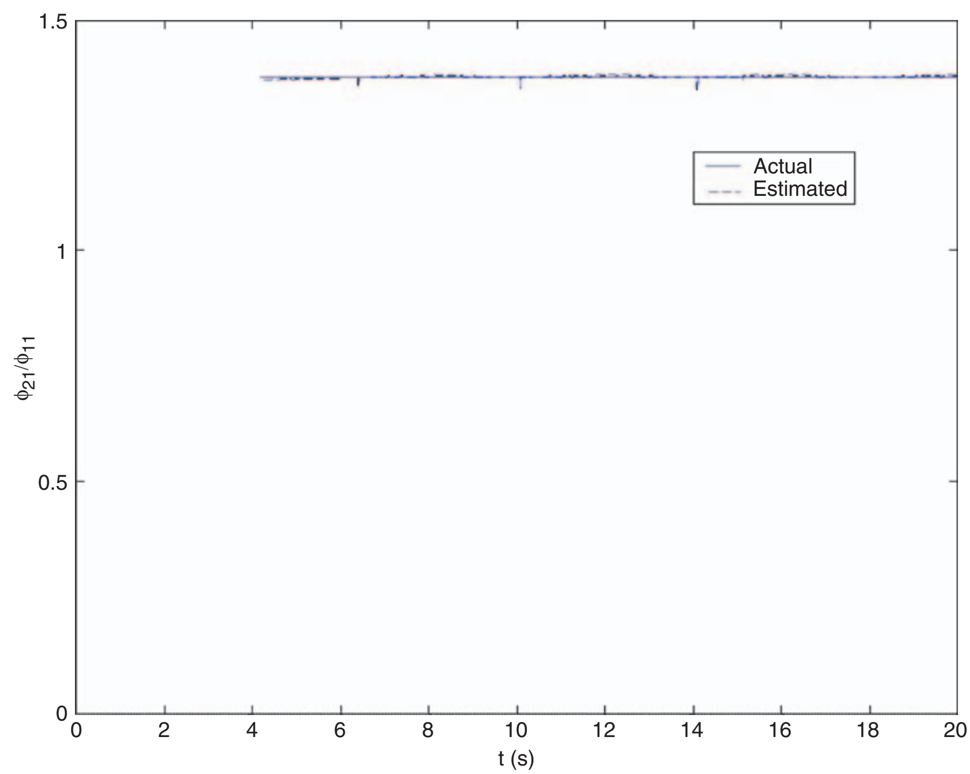

Figure 7 Online tracking of fundamental mode shape of a 2 DOF system.

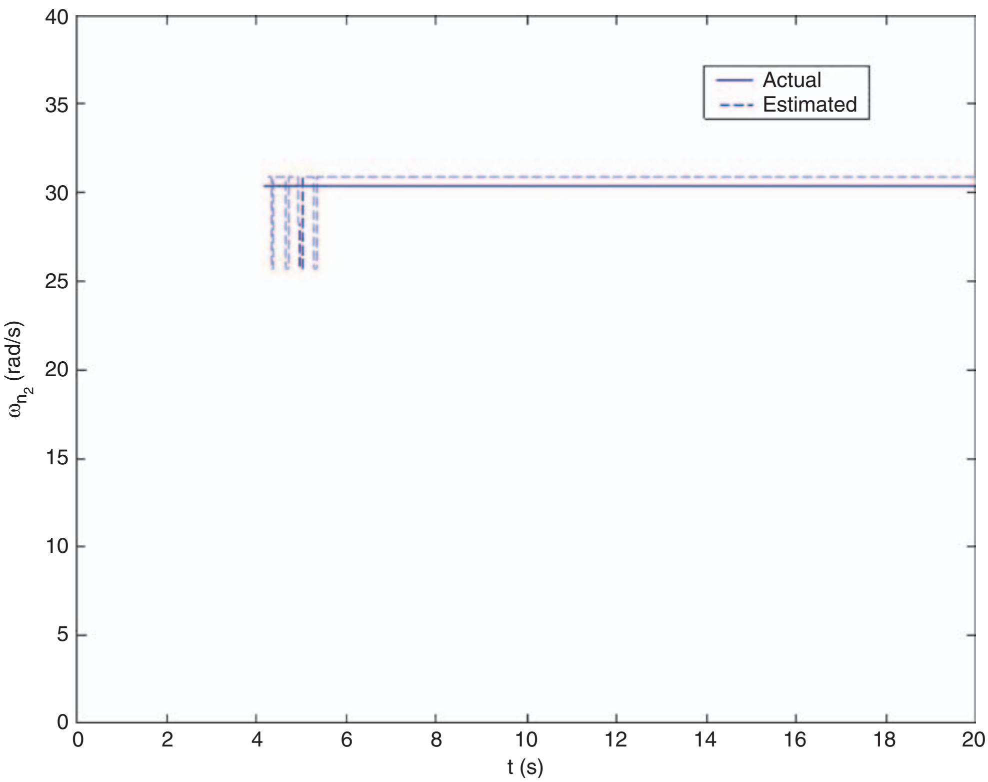

Figure 8 Online tracking of second natural frequency of a 2 DOF system.

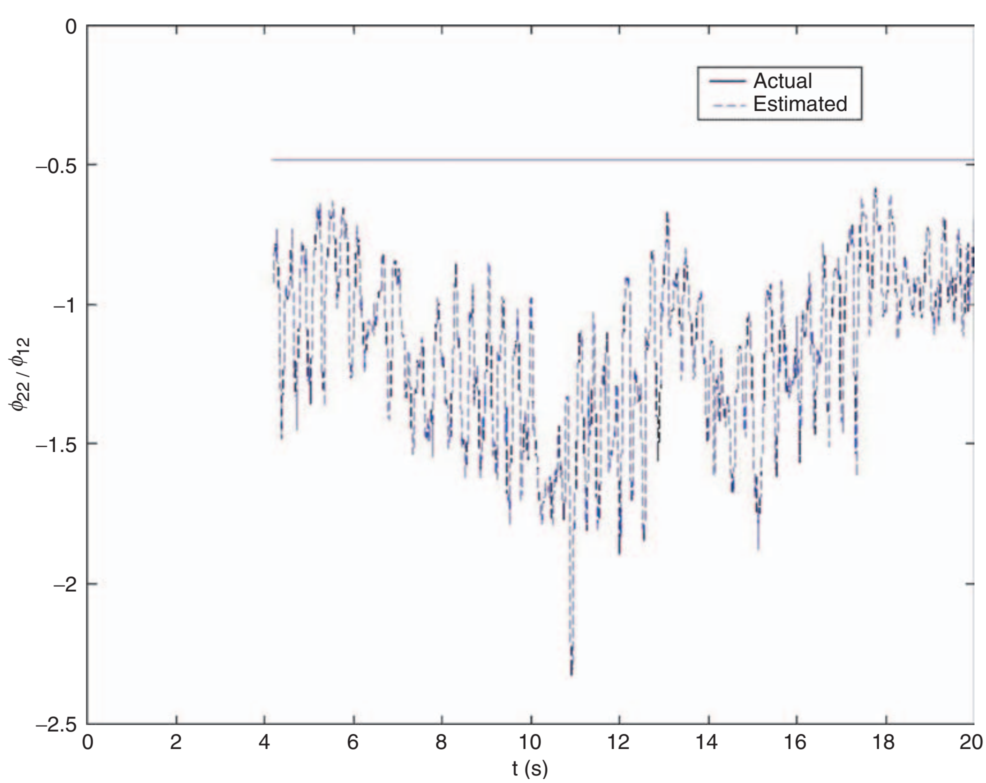

Figure 9 Online tracking of second mode shape of a 2 DOF system.

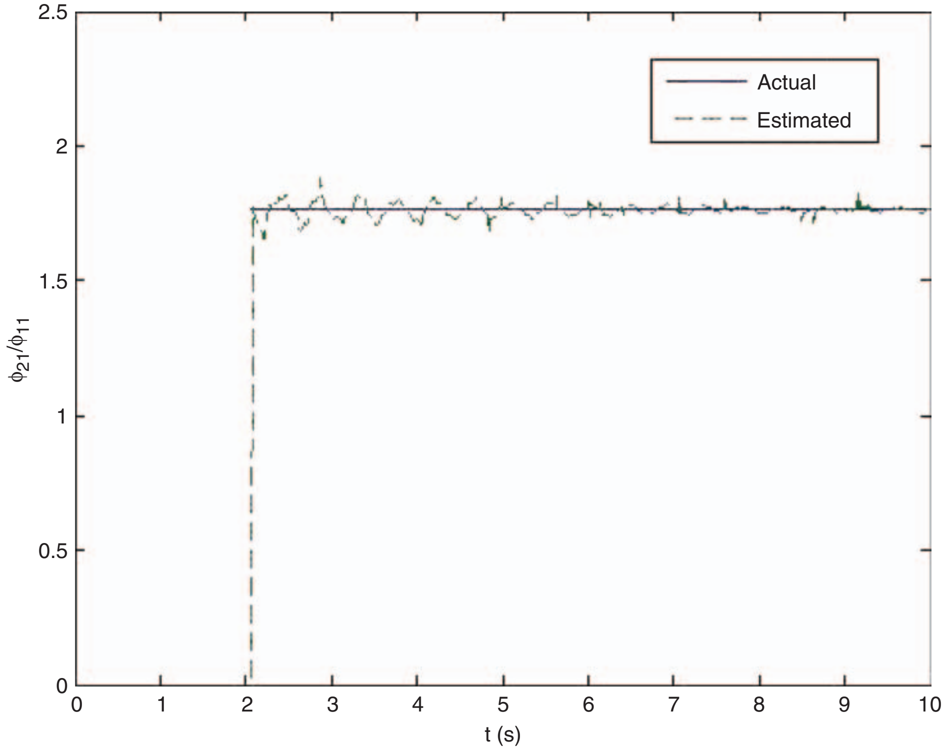

Figure 10 Online tracking of the second mode shape value at second node for a 5 DOF system.

$m_2 = 20$ unit, $m_3 = 20$ unit, $m_4 = 25$ unit, and $m_5 = 35$ unit, respectively. The floor stiffness from the first to the fifth are $k_1 = 15000$ unit, $k_2 = 20000$ unit, $k_3 = 36000$ unit, $k_4 = 24000$ unit, and $k_5 = 36000$ unit, respectively. A uniform modal damping of 1% has been assumed. The structure is assumed to be excited by an arbitrary initial condition $\{X(0)\}=\{1.0\ \ 1.8\ \ 1.7\ \ 0.6\ \ -1.5\}$ unit to increase the possibility of excitation of the second mode. A window with 200 time points at an interval of 0.0104 s leading to a time delay of 2.08 s and the parameters $F_1 = 8.5$ rad/s and $\sigma = 1.2$ are used. It has been observed that the second natural frequency and the second mode shape are successfully tracked. As a representative plot, the online tracking of the second mode shape value for the second degree of freedom (second floor) is shown in Figure 10. In order to examine the ability of the proposed method to online identify system parameters in cases when excited by transient, non-white excitations; an amplitude modulated non-stationary excitation is further considered. A band limited excitation to cover the range of frequencies to be excited is simulated and modulated by a Shinozuka and Sato [36] type of amplitude modulating function (with parameters $\alpha = 4$, $\beta = 6.22$, and $\gamma = 3.11$ leading to a peak of the modulating function at around 4.99 s) to generate a transient excitation. The 5 DOF structure is subjected to this base excitation with the first mode primarily excited and hence dominating the response. The proposed tracking algorithm is able to track the first mode accurately.

To further observe if the proposed method can track a sudden change in the stiffness(es) of an MDOF system and follow the recovery to the original stiffness value(s) the stiffnesses k_1 and k_2 of the 2 DOF are changed to 5000 and 5200 unit, respectively at an instant of 5.72 s in time. Subsequently, the stiffnesses are restored to their original value at 12.48 s. During the changed phase the natural frequencies and the mode shapes are changed to $\omega_1 = 11.57$ rad/s; $\omega_2 = 35.11$ rad/s; and $\{\phi_{11}\ \ \phi_{21}\}^t = \{1\ \ 1.57\}$; $\{\phi_{12}\ \ \phi_{22}\}^t = \{1\ \ -0.48\}$. Figures 11 and 12 show the tracked first natural frequency and the ratio of ϕ_{21}/ϕ_{11}. As observed earlier, there

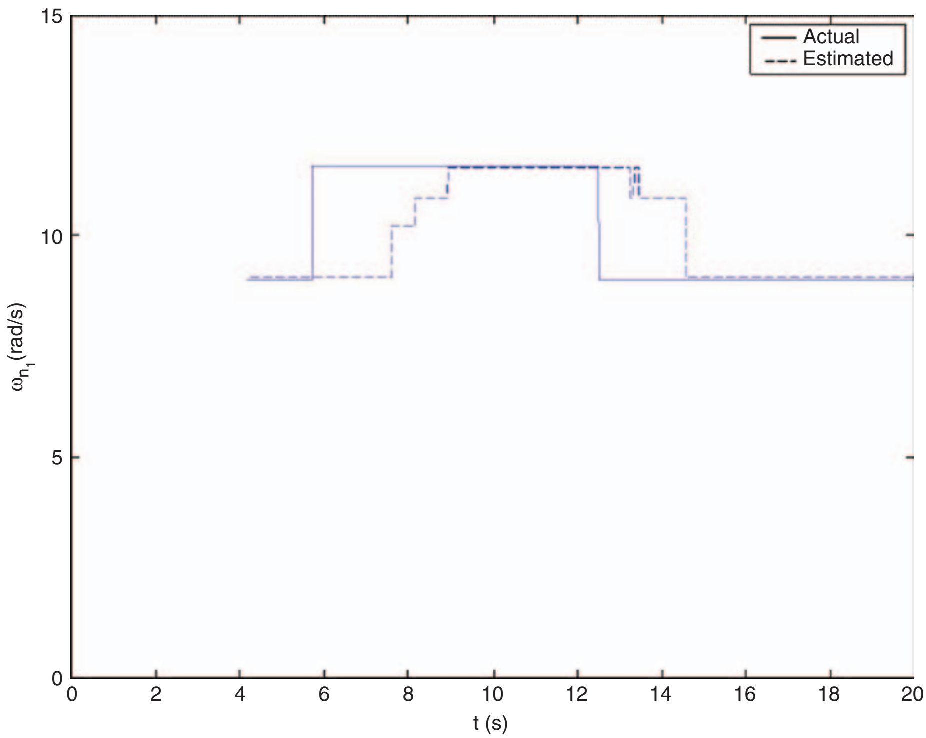

Figure 11 Online tracking of fundamental frequency of a 2 DOF system with sudden change and subsequent restoration in stiffness.

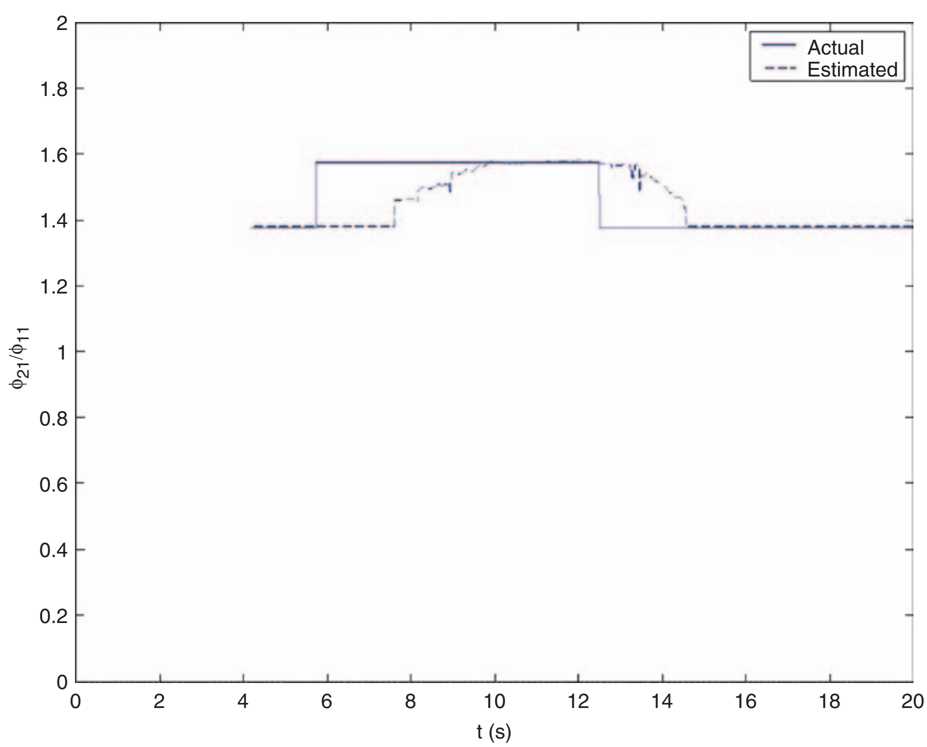

Figure 12 Online tracking of fundamental mode shape of a 2 DOF system with sudden change and subsequent restoration in stiffness.

is a time lag in tracking the frequency and mode shape. The change in the frequency is tracked in (three) steps corresponding to the bands of frequencies considered. The second modal estimates are poor as was observed earlier and is not unexpected as discussed earlier.

4 Conclusions

A wavelet based online structural dynamic parameter identification method has been proposed. The developed theory can identify online variation in natural frequency of a SDOF system and the natural frequencies and mode shapes of a MDOF system arising out of change in stiffness(es). A modified L–P wavelet basis function has been used and has the advantage of adapting for wavelet packets for desired accuracy in estimation. The analytical results confirm the ability of the technique to track in several cases of stiffness variation considered here. The proposed algorithm is versatile as it has the ability to detect changes over a shorter time scale (due to a sudden event/failure) in addition to track changes due to long-term phenomenon, such as fatigue. The proposed method is simple and easy to implement for online identification and vibration control of stiffness varying structural systems.

References

1. Adams, D.E. and Allemang, R.J. (2000). A frequency domain method for estimating the parameters of a non-linear structural dynamic model through feedback. *Mech. Syst. Signal Process*, *14*(*4*), 637–656.
2. Basu, B. (2005). Identification of stiffness degradation in structures using wavelet analysis. *Journal of Construction and Building Material*, *19*, 713–721.
3. Basu, B. (2004). Wavelet analysis for identification of stiffness degradation. *7th International Conf. Railway Engineering*, London, CD-ROM.
4. Basu, B. and Gupta, V.K. (1999). A non-stationary response of MDOF systems by wavelet transform. *Earthquake Engineering and Structural Dynamics*, *26*, 1243–1258.
5. Basu, B. and Gupta, V.K. (1998). Seismic response of SDOF system by wavelet modeling of non-stationary processes. *Journal of Engineering Mechanics*, *ASCE*, *124*(*10*), 1142–1150.
6. Beck, J.L. (1980). Structural identification using linear models and earthquake records. *Earthquake Engineering and Structural Dynamics*, *8*, 145–160.
7. Bendat, J. (1990). *Nonlinear System Analysis and Identification from Random Data*, New York: Wiley.
8. Chatterjee, P. and Basu, B. (2004). Wavelet based non-stationary seismic rocking response of flexibly supported tanks. *Earthquake Engineering and Structural Dynamics*, *33*, 157–181.
9. Chatterjee, P. and Basu, B. (2006). Non-stationary seismic response of a tank on a bilinear hysteretic soil using wavelet transform. *Probabilistic Engineering Mechanics*, *21*(*1*), 54–63.
10. Doebling, S.W., Farrar, C.R. and Prime, M.B. (1998). A summary review of vibration-based identification methods. *Shock and Vibration Digest*, *205*, 631–645.
11. Dharap, P., Koh, B.H. and Nagarajaiah, S. (2006). Structural health monitoring using ARMarkov observers. *Journal of Intelligent Material Systems and Structures*, *17*(*6*), 469–481.
12. Ghanem, R. and Shinozuka, M. (1995). Structural system identification. I: Theory. *Journal of Engineering Mechanics*, *ASCE*, *121*(*2*), 255–264.
13. Ghanem, R. and Romeo, F. (2000). A wavelet based approach for the identification of linear time-varying dynamical systems. *Journal of Sound and Vibration*, *234*(*4*), 555–576.
14. Ghanem, R. and Romeo, F. (2001). A wavelet based approach for model and parameter identification of non-linear systems. *Non-linear Mechanics*, *36*, 835–859.
15. Hoshiya, M. and Saito, E. (1984). Structural identification by extended Kalman filtering. *Journal of Engineering Mechanics*, *ASCE*, *110*, 1757–1770.
16. Hart, G.C. and Yao, J.T.P. (1977). System identification in structural dynamics. *Journal of Engineering Mechanics*, *ASCE*, *103*(*6*), 1089–1104.
17. Katida, Y. (1998). Identification of nonlinear structural dynamic systems using wavelets. *Journal of Engineering Mechanics*, *ASCE*, *124*(*10*), 1059–1066.
18. Koh, B.H., Li, Z., Dharap, P., Nagarajaiah, S. and Phan, M.Q. (2005a). Actuator failure detection through interaction matrix formulation. *Journal of Guidance*, *Control*, *and Dynamics*, *AIAA*, *28*(*5*), 895–901.
19. Koh, B.H., Dharap, P., Nagarajaiah, S. and Phan, M.Q. (2005b). Real-time structural damage monitoring by input error function. *Journal of American Institute of Aeronautics and Astronautics*, *AIAA*, *43*(*8*), 1808–1814.
20. Kozin, F. and Natke, H.G. (1986). System identification technique. *Structural Safety*, *3*, 269–316.
21. Lardies, J. and Gouttebroze, S. (2002). Identification of modal parameters using the wavelet transform.

International Journal of Mechanical Science, *44*, 2263–2283.
22. Lin, C.C., Soong, T.T and Natke, H.G. (1990). Real time system identification of degrading structures. *Journal of Engineering Mechanics*, *ASCE*, *116*(*10*): 2258–2274.
23. Liu, K. (1997). Identification of linear time-varying systems. *Journal of Sound and Vibration*, *206*, 487–505.
24. Masri, S.F. and Caughey, T.K. (1979). A nonparametric identification technique for nonlinear dynamic problems. *Journal of Applied Mechanics*, *46*, 433–447.
25. Nagarajaiah, S., Riley, M.A. and Reinhorn, A. (1993). Control of sliding-isolated bridge with absolute acceleration feedback. *Journal of Engineering Mechanics*, *ASCE*, *119*(*11*), 2317–2332.
26. Nagarajaiah, S. and Nadathur, V. (2005). Semi-active control of wind excited building with variable stiffness TMD using short time Fourier transform. *Engineering Structures*, *27*, 431–441.
27. Newland, D.E. (1983). *An Introduction to Random Vibration*, *Spectral and Wavelet Analysis*. UK: Longman.
28. Newland, D.E. (1994). Wavelet analysis of vibration, Part I: Theory, Part II: Wavelet maps. *Journal of Vibration and Acoustics*, *Transactions of ASME*, *116*, 409–425.
29. Newland, D.E. (1993). Harmonic wavelet analysis. *Proceedings of the Royal Society of London* (*A*), *443*, 203–225.
30. Patten, W.N., Sack, R.L. and He, Q. (1996). Controller semiactive hydraulic vibration absorber for bridges. *Journal of Structural Engineering*, *ASCE*, *122*, 187–192.
31. Piombo, B.A.D., Fasana, A., Marchesiello, S. and Ruzzene, M. (2000). Modelling and identification of the dynamic response of a supported bridge. *Mechanical Systems and Signal Processing*, *14*(*1*), 75–89.
32. Richards, C.M. and Singh, R. (1998). Identification of multi-degree-of-freedom non-linear systems under random excitations by the ''reverse path'' spectral method. *Journal of Sound and Vibration*, *213*(*4*), 673–708.
33. Staszewski, W.J. (1997). Identification of damping in MDOF system using time-scale decomposition. *Journal of Sound and Vibration*, *203*(*2*), 283–305.
34. Staszewski, W.J. (1998). Identification of non-linear systems using multi scale ridges and skeleton of wavelet transform. *Journal of Sound and Vibration*, *214*(*4*), 639–658.
35. Shinozuka, M. and Ghanem, R. (1994). Structural system identification. II: Experimental verification. *Journal of Engineering Mechanics*, *ASCE*, *121*(*2*), 265–273.
36. Shinozuka, M. and Sato, Y. (1967). Simulation of nonstationary random processes. *Journal of Engineering Mechanics*, *ASCE*, *93*(*1*): 11–40.
37. Spencer, B. and Nagarajaiah, S. (2003). State of the art of structural control. *Journal of Engineering Mechanics*, *ASCE*, *129*(*7*): 845–856.
38. Smyth, A.W., Masri, S.F., Chassiakos, A.G. and Caughey, T.K. (1999). On-line parametric identification of MDOF non-linear hysteretic systems. *Journal of Engineering Mechanics*, *ASCE 125*(*2*), 133–142.
39. Soong, T.T. (1990). *Active Structural Control: Theory and Practice*, New York: Longman.
40. Spencer, B.F., Suhardjo, J. and Sain, M.K. (1994). Frequency domain optimal control for aseismic protection. *Journal of Engineering Mechanics*, *ASCE*, *120*(*1*), 135–159.
41. Spina, D., Valente, C. and Tomlinson, G.R. (1996). A new procedure for detecting non-linearity from transient data using the Gabor transform. *Nonlinear Dynamics*, *11*, 235–254.
42. Sae-Ung, S. and Yao, J.T.P. (2004). Active control of building structures. *Journal of Engineering Mechanics*, *ASCE*, *104*(*2*), 335–350.
43. Tratskas, P. and Spanos, P.D. (2003). Linear multi-degree-of-freedom stochastic response by using the wavelet transform. *Journal of Applied Mechanics*, *ASME*, *70*(*5*),724–731.
44. Udwadia, F.E. and Jerath, N. (1980). Time variations of structural properties during strong ground shaking. *Journal of Engineering Mechanics*, *ASCE*, *106*, 11–121.
45. Varadarajan, N. and Nagarajaiah, S. (2004). Wind response control of building with variable stiffness tuned mass damper using empirical model decomposition/Hilbert transform. *Journal of Engineering Mechanics*, *ASCE*, *130*(*4*), 451–458.
46. Worden, K. and Tomlinson, G.R. (2001). *Nonlinearity in Structural Dynamics*, Institute of Physics, London.
47. Wu, J.C. and Yang, J.N. (1998). Active control of transmission tower under stochastic wind. *Journal of Structural Engineering*, *ASCE*, *124*(*11*), 1302–1312.
48. Yang, J.N. and Samali, B. (1983). Control of tall buildings in along-wind motion. *Journal of Structural Engineering*, *ASCE*, *109*(*1*), 50–68.
49. Yang, J.N., Akbarpour, A. and Ghaemmaghami, P. (1987). New optimal control algorithms for structural control. *Journal of Engineering Mechanics*, *ASCE*, *113*(*9*), 1369–1386.
50. Yang, J.N., Li, Z. and Liu, S.C. (1992). Stable controllers for instantaneous optimal control. *Journal of Engineering Mechanics*, *ASCE*, *118*(*8*), 1612–1630.

51. Yang, Y.N., Wu, J.C. and Agrawal, A.K. (1995a). Sliding mode control for seismically excited linear structures. *Journal of Engineering Mechanics*, *ASCE*, *121*(*12*), 1386–1390.
52. Yang, Y.N., Wu, J.C. and Agrawal, A.K. (1995b). Sliding mode control for nonlinear and hysteretic structures. *Journal of Engineering Mechanics*, *ASCE*, *121*(*12*), 1330–1339.
53. Yang, J.N., Agarwal, A., Samali, B. and Wu, J.C. (2004). Benchmark problem for response control of wind-excited tall buildings. *Journal of Engineering Mechanics*, *ASCE*, *130*(*4*), 437–446.
54. Yang, C., Adams, D.E. and Ciray, S. (2005). System identification of nonlinear mechanical systems using embedded sensitivity functions. *Journal of Vibration and Acoustics*, *Transactions of ASME*, *127*(*6*), 530–541.